

# Study of elastic scattering cross-sections of $^{14}\text{N}$ by $^{56}\text{Fe}$

Kamala Kanta Jena<sup>\*1</sup>, Dibyaranjan Sha<sup>1</sup>, B. B. Sahu<sup>2</sup>, S. K. Agarwalla<sup>3</sup>

<sup>1</sup>P. G. Department of Physics, Bhadrak Autonomous College, Bhadrak, Odisha-756100, India

<sup>2</sup>School of Applied Sciences, KIIT Deemed to be University, Bhubaneswar 751024, India

<sup>3</sup>P. G. Department of Physics, Fakir Mohan University, Balasore, Odisha -756019, India

Emails : [kkjena1@gmail.com](mailto:kkjena1@gmail.com); [dibyanjanfmu@gmail.com](mailto:dibyanjanfmu@gmail.com); [bbsahufpy@kiit.ac.in](mailto:bbsahufpy@kiit.ac.in); [santosh.iopb@gmail.com](mailto:santosh.iopb@gmail.com)

## Introduction

We use a phenomenological optical potential developed in light of a versatile potential designed by J. N. Ginocchio. We use the potential to explain angular distribution of experimental scattering cross-sections in wide ranges of angle and energy. The present paper discusses the study of elastic scattering cross-sections of the system  $^{14}\text{N}+^{56}\text{Fe}$  near Coulomb barrier. Our theoretical predictions are well competitive with the experimental data.

## Theoretical Formulation

Particles with a mass greater than He-4 and one or more units of electronic charge are called heavy-ions. Heavy-ion collisions deal with nuclei of large mass and big size. We frame a nuclear potential by using versatile Ginocchio potential [1] by developing algorithm in *FORTTRAN* to study heavy-ion elastic collisions. The effective potential  $V_{\text{eff}}(r)$  contains nuclear potential  $V_N(r)$ , Coulomb potential  $V_C(r)$  and centrifugal part as represented by Eq.1.

$$V_{\text{eff}}(r) = V_N(r) + V_C(r) + l(l+1)\hbar^2/2\mu r^2 \quad \dots (1)$$

The nuclear potential  $V_N(r)$  is complex in nature and described as  $V_N(r) = V_n(r) + i W_n(r)$ , where  $V_n(r)$  is the real part and  $W_n(r)$  is the imaginary part. The real part  $V_n(r)$  is described [2,3] by Eq.2.

$$V_n(r) = \begin{cases} -\frac{V_B}{B_1} \left[ B_0 + \frac{(B_1 - B_0)}{\cosh^2 \rho_1} \right], & \text{if } 0 < r < R_0 \\ -\frac{V_B}{B_2} \left[ \frac{B_2}{\cosh^2 \rho_2} \right], & \text{if } r \geq R_0 \end{cases} \quad (2)$$

The real part has volume region ( $r < R_0$ ) and surface region ( $r \geq R_0$ ). Imaginary part  $W_n(r)$  has similar form as that of real part, but weaker in strength. Here  $\rho_1 = (r - R_0)b_1$  and  $\rho_2 = (r - R_0)b_2$ .  $R_0$  is the radial distance in surface region; slope  $b_n = \sqrt{\frac{2\mu V_B}{\hbar^2 B_n}}$ , reduced mass  $\mu = \frac{m_T m_P}{m_T + m_P}$  and  $V_B$  is barrier height at  $r = R_0$ . Parameter  $B_0$  controls potential depth at the origin  $r = 0$ , whereas, parameter  $V_B$  is related to the potential depth at  $R_0$  position.  $V_B$  controls parameter  $b_n$  as well. The slope parameter  $b_n$  is also affected by parameter  $B_n$  on either side of  $R_0$ .

Interacting projectile (P) and target (T) behave as a uniformly charged sphere of radius,  $R_C = r_C (A_P^{1/3} + A_T^{1/3})$ . Coulomb potential  $V_C(r)$  for the interacting nuclei is given by

$$V_C(r) = \begin{cases} \frac{Z_P Z_T e^2}{2 R_C^3} (3R_C^2 - r^2), & \text{if } r < R_C \\ \frac{Z_P Z_T e^2}{r}, & \text{if } r \geq R_C \end{cases} \quad (3)$$

The last term in Eq.1 may be neglected for  $l = 0$ . With the above effective potential we solve Schrodinger equation to obtain total scattering amplitude  $f(\theta) = f_C(\theta) + f_N(\theta)$ , i.e., sum of Coulomb scattering amplitude  $f_C(\theta)$  and nuclear scattering amplitude  $f_N(\theta)$ . The ratio of elastic cross-section ( $\sigma_{el}$ ) with respect to Rutherford cross-section ( $\sigma_{\text{Ruth}}$ ) is given [2-7] as

$$\frac{d\sigma_{el}}{d\sigma_{\text{Ruth}}} = \left| \frac{f(\theta)}{f_C(\theta)} \right|^2 \quad \dots \dots (4)$$

The cross-section  $\sigma_{el}$  for  $l^{\text{th}}$  partial wave with the S-matrix  $S_l$  may be expressed as

$$\sigma_{el} = \frac{\pi}{k^2} (2l+1) |1 - S_l|^2 \quad \dots \dots (5)$$

Wave vector  $k$  is given by,  $k = \sqrt{\frac{2\mu E}{\hbar^2}}$ .

\* Corresponding Author : [kkjena1@gmail.com](mailto:kkjena1@gmail.com)

## Results And Discussions

Real part of the effective optical potential for  $l=0$  is shown in Fig.1 at  $E_{CM} = 22.4$  MeV with  $R_0=9.4$ fm,  $B_1=4.0$ ,  $B_2=0.01$ ,  $B_0=29.99$ MeV,  $V_B=2.8$ MeV,  $R_{0W}=9.5$ fm,  $W_1=1.1$ ,  $W_2=0.28$ ,  $W_0=1.6$ MeV &  $V_{BW}=0.7$ MeV. There is a transition in the potential around  $r = 9.4$  fm. This is known as *non-trivial behavior*. This behavior helps us explain experimental result within a wide range of incident energy.

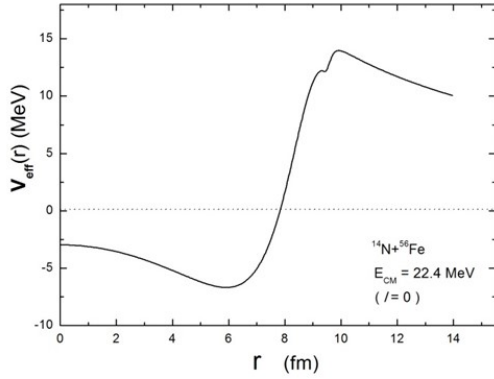


Fig.1 : Real part of the effective potential

We apply formalism to study angular cross-sections of the elastic scattering system  $^{14}\text{N}+^{56}\text{Fe}$  in the energy range from 22.4 to 32 MeV. To explain the experimental observations, best-fit parameters of the optical potential are given in Table-I. Colliding energy in centre of mass frame ( $E_{CM}$ ), potential parameters  $V_B$ ,  $B_0$  and  $V_{BW}$  have the same unit in MeV. Theoretical cross-sections (solid line curve) are compared with experimental values (solid spheres) performed by Williams et al. [8]. Experimental data for the system are obtained from site <http://nrv.jinr.ru>. Energy independent parameters are found to be  $R_0=9.4$  fm,  $R_{0W}=9.5$  fm,  $B_1=4.0$ ,  $W_0=1.6$  MeV,  $W_1=1.1$  and  $W_2=0.28$  for the entire range of energies.

Table-I : Energy-dependent parameters

$E_{CM}$	$V_B$	$B_0$	$B_2$	$V_{BW}$
22.4	2.8	29.99	0.01	0.7
25.6	3.8	26.99	0.15	1.2
28.8	2.4	22.49	0.17	1.4
32.0	2.1	20.99	0.095	1.4

The theoretical values fairly explain the experimental observations for all energies. Fig.2 depicts such an agreement at incident energy 32 MeV in centre of mass frame.

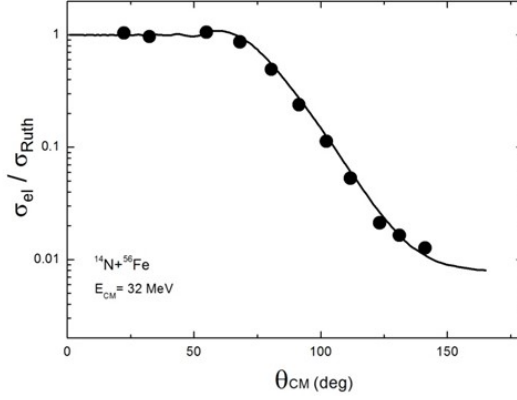


Fig.2 : Plot of theoretical cross-sections against experimental values for  $^{14}\text{N}+^{56}\text{Fe}$  at 32 MeV

## Conclusion

The potential has a versatility to fairly explain experimental observations in a wide range of energies. The potential has also explained experimental data for a wide range of systems with light as well as heavy projectiles. The present work can be extended to study the phenomena of threshold anomaly and breakup threshold anomaly near Coulomb barrier.

## References

- [1] J. N. Ginocchio, Ann. Phys. 152 (1984) 203
- [2] G.S. Mallick, S.K. Agarwalla, B. Sahu et al., Phys.Rev.C 73 (2003) 054606
- [3] K. K. Jena, S. K. Agarwalla and B. B. Sahu, New J. Phys. 25 (2023) 033012
- [4] K. K. Jena, S. K. Agarwalla and B. B. Sahu, Acta Phys. Pol.B, 53, 10-A1 (2022)
- [5] K. K. Jena, B. Sahu, Jajati K. Nayak et al., Acta Phys. Pol.B, 54, 4-A1 (2023)
- [6] K. K. Jena, B. B. Sahu and S. K. Agarwalla, Proc. DAE Symp. Nucl. Phys. 66 (2022) 662
- [7] K. K. Jena, B. B. Sahu and S. K. Agarwalla, Proc. DAE Symp. Nucl. Phys. 67 (2023) 703
- [8] M. E. Williams, R. H. Davis, C. I. Delaune, et al., Phys. Rev. C 11, 906 (1975).